3-19-2020

Quantum Critical Point in the Itinerant Ferromagnet Ni1-xRhx

C.-L. Huang

A M. Hallas

K Grube

S Kuntz

B Spiess

See next page for additional authors

Recommended Citation

Huang, C-L., A. M. Hallas, K. Grube, S. Kuntz, B. Spieß, K. Bayliff, T. Besara et al. "Quantum Critical Point in the Itinerant Ferromagnet Ni 1− x Rh x." Physical review letters 124, no. 11 (2020): 117203.

Authors

C.-L. Huang; A M. Hallas; K Grube; S Kuntz; B Spiess; K Bayliff; Tiglet Besara; T Siegrist; and For complete list of authors, see publisher's website.

Quantum Critical Point in the Itinerant Ferromagnet $Ni_{1-x}Rh_x$

C.-L. Huang,[1,*] A. M. Hallas,[1,2] K. Grube,[3] S. Kuntz,[3] B. Spieß,[1,4] K. Bayliff,[5] T. Besara,[6,7]
T. Siegrist,[6,10] Y. Cai,[8] J. Beare,[8] G. M. Luke,[8,9] and E. Morosan[1]
[1]*Department of Physics and Astronomy, Rice University, Houston, Texas 77005, USA*
[2]*Department of Physics and Astronomy and Quantum Matter Institute, University of British Columbia, Vancouver, British Columbia V6T 1Z1, Canada*
[3]*Institute for Quantum Materials and Technologies, 76021 Karlsruhe, Germany*
[4]*Department of Chemistry, Johannes Gutenberg-University Mainz, 55131 Mainz, Germany*
[5]*Department of Chemistry, Rice University, Houston, Texas 77005, USA*
[6]*National High Magnetic Field Laboratory, Tallahassee, Florida 32310, USA*
[7]*Department of Physics, Astronomy, and Materials Science, Missouri State University, Springfield, Missouri 65897, USA*
[8]*Department of Physics and Astronomy, McMaster University, Hamilton, Ontario L8S 4M1, Canada*
[9]*TRIUMF, 4004 Wesbrook Mall, Vancouver, British Columbia V6T 2A3, Canada*
[10]*FAMU-FSU College of Engineering, Tallahassee, Florida 32310, USA*

(Received 15 January 2020; accepted 26 February 2020; published 19 March 2020)

We report a chemical substitution-induced ferromagnetic quantum critical point in polycrystalline $Ni_{1-x}Rh_x$ alloys. Through magnetization and muon spin relaxation measurements, we show that the ferromagnetic ordering temperature is suppressed continuously to zero at $x_{\mathrm{crit}} = 0.375$ while the magnetic volume fraction remains 100% up to x_{crit}, pointing to a second order transition. Non-Fermi liquid behavior is observed close to x_{crit}, where the electronic specific heat C_{el}/T diverges logarithmically, while immediately above x_{crit} the volume thermal expansion coefficient α_V/T and the Grüneisen ratio $\Gamma = \alpha_V/C_{\mathrm{el}}$ both diverge logarithmically in the low temperature limit, further indication of a ferromagnetic quantum critical point in $Ni_{1-x}Rh_x$.

DOI: 10.1103/PhysRevLett.124.117203

A quantum critical point (QCP) occurs when a phase transition is continuously suppressed to zero temperature. The intense quantum fluctuations in the vicinity of a QCP profoundly alter a material's electronic properties, resulting in non-Fermi liquid behavior and, in some cases, unconventional superconductivity [1,2]. The most ubiquitous QCP separates an antiferromagnetically ordered state from one in which quantum fluctuations disrupt the order. Notable examples are found among heavy fermion systems [1,3,4]. QCPs in ferromagnetic (FM) metals have proven far more elusive [5]. It is now understood that a FM QCP is inherently unstable and can survive only in rare circumstances [6]. In this Letter, we report the discovery of a FM QCP in $Ni_{1-x}Rh_x$, as evidenced by (i) a second-order phase transition up to the critical concentration x_{crit}, and (ii) divergence of the electronic specific heat coefficient C_{el}/T, the volume thermal expansion α_V/T, and the Grüneisen ratio $\Gamma = \alpha_V/C_{\mathrm{el}}$. The dilution of the *d*-electron magnetic sublattice as the tuning parameter to induce a FM QCP opens a new route for exploring FM quantum criticality and possible new collective phases near the QCP, such as unconventional superconductivity [7].

FM QCPs are revealed via chemical substitution in $Zr_{1-x}Nb_xZn_2$ [8], $SrCo_2(Ge_{1-x}P_x)_2$ [9], $YbNi_4(P_{1-x}As_x)_2$ [10], and $(Sc_{1-x}Lu_x)_{3.1}In$ [11]. The disorder effect is minimal or negligible in these systems. For $SrCo_2(Ge_{1-x}P_x)_2$, the QCP is induced by the breaking of dimers [9]. However, the exact mechanism responsible for the FM QCP in the other three systems remains unclear. In most other FM metals, the QCP is preempted when the continuous (second-order) transition as a function of nonthermal control parameter either becomes discontinuous (first order), or the ferromagnetism is replaced by a spatially modulated ordered state [5,12–15]. Theoretical work by Belitz, Kirkpatrick, and Vojta (BKV) has proposed a route towards a FM QCP by long-range effective spin interactions that occur in the presence of quenched disorder [6,16,17]. A handful of FM QCPs have been identified as candidates for this phenomenology, including $UCo_{1-x}Fe_xGe$ [18], $(Mn_{1-x}Fe_x)Si$ [19], $NiCoCr_x$ [20], and $Ce(Pd_{1-x}Ni_x)_2P_2$ [21], where disorder is inherently introduced by the chemical substitution. In most of these systems, the proposed existence of a QCP is based on either divergence of some thermodynamic parameters [18,20,21] or the second-order nature of the transition [19]. However, the unambiguous identification of a QCP requires that both these criteria be fulfilled. This point is exemplified by disordered $Sr_{1-x}Ca_xRuO_3$, for which a QCP can be ruled out because the transition at $T = 0$ is first order [22], and yet, quantum critical scaling is still observed [23]. Thus, in order to unambiguously identify a FM QCP it is essential that both thermodynamic signatures of quantum fluctuations *and* second-order behavior be observed simultaneously. Our observation of both these requisite signatures in a chemically simple material where the FM QCP is induced via direct dilution of its *d* electrons elevate $\mathrm{Ni}_{1-x}\mathrm{Rh}_x$ to a top tier of candidates.

Elemental Ni, which has a simple face-centered cubic structure, is known to order ferromagnetically below its Curie temperature $T_C = 627$ K [24]. Upon alloying with Rh, the T_C of $\mathrm{Ni}_{1-x}\mathrm{Rh}_x$ is quickly suppressed [25]. $\mathrm{Ni}_{1-x}\mathrm{Rh}_x$ has more configuration entropy than pure Ni [26]. Also, the metallic radii of Ni (124 pm) and Rh (134 pm) differ by ~8%. Naturally, one would expect that, compared to pure Ni, there is more disorder in $\mathrm{Ni}_{1-x}\mathrm{Rh}_x$ alloy, making it a good candidate to test for the existence of a disorder-driven FM QCP. Polycrystalline $\mathrm{Ni}_{1-x}\mathrm{Rh}_x$ samples with $0.3 \leq x \leq 0.42$ were prepared by arc melting the constituents Ni and Rh and annealed at 1000 °C. Magnetization measurements were carried out using a Quantum Design (QD) magnetic property measurement system. Zero-field muon spin relaxation measurements were performed at the M20 surface muon channel at TRIUMF. Specific heat was measured using a QD Dynacool physical property measurement system equipped with a dilution refrigerator. Thermal expansion was measured with a homemade capacitance dilatometer. More details about the sample characterizations and experimental methods are provided in the Supplemental Material [27–34].

Figure 1(a) shows the $\mu_0 H = 0.01$ T magnetic susceptibility $\Delta M(T)/H$ of $\mathrm{Ni}_{1-x}\mathrm{Rh}_x$, after a temperature-independent contribution M_0 was subtracted from the measured $M(T)$ $(\Delta M = M - M_0)$. $\Delta M/H$ sharply increases as T is lowered through T_C for $x = 0.32$–0.36 where T_C is determined both through a linear fit, as shown in Fig. 1(a), and the Arrott-Noakes analysis as discussed below. For $x_{\mathrm{crit}} = 0.375$ (where $T_C \to 0$), $\Delta M/H$ shows only a small increase down to the lowest measured temperature of 2 K, consistent with the complete suppression of FM order. Isothermal magnetization measurements at $T = 2$ K confirm that $\mathrm{Ni}_{1-x}\mathrm{Rh}_x$ is a soft ferromagnet without a measurable hysteresis [Fig. 1(b)]. We cannot rule out a very small antiferromagnetic component or canting close to x_{crit}, although magnetization suggests that FM correlations dominate, as evidenced by an abrupt increase of $M(H)$ at the lowest field [Fig. 1(b)] and adherence to Arrott-Noakes scaling all the way up to x_{crit}. Future neutron scattering and nuclear magnetic resonance measurements will shed light on this issue. For the $x = 0.32$ sample, which orders near 100 K, the inverse magnetic susceptibility $H/\Delta M$ exhibits Curie-Weiss-like behavior between 150 and 300 K, from which we derive a paramagnetic (PM) effective moment $\mu_{\mathrm{PM}} = 1.97\mu_B/\mathrm{f.u.}$ (see the Supplemental Material [27]). For the same sample, ΔM is small at 7 T ($\sim 0.22\mu_B/\mathrm{f.u.}$), and the Rhodes-Wohlfarth ratio, $\mu_{\mathrm{PM}}/\mu_{\mathrm{sat}} = 9$, much larger than unity, is indicative of itinerant moment behavior in $\mathrm{Ni}_{1-x}\mathrm{Rh}_x$ [35].

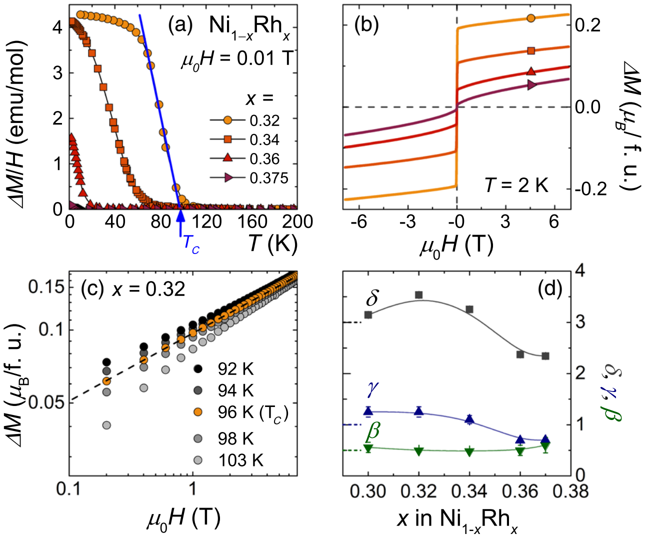

FIG. 1. (a) Magnetic susceptibility $\Delta M/H = (M - M_0)/H$ for $\mu_0 H = 0.01$ T and (b) isothermal magnetization ΔM at $T = 2$ K of $\mathrm{Ni}_{1-x}\mathrm{Rh}_x$. Solid line in (a) shows how T_C was determined. (c) Log-log magnetization isotherms for $x = 0.32$, with the dashed line showing T_C. (d) Critical exponents β, γ, and δ determined from the Arrott-Noakes scaling plots as a function of x. Solid lines are guides to the eye. Mean-field values $\beta = 0.5$, $\gamma = 1$, and $\delta = 3$ are indicated by horizontal dashed lines.

An earlier study indicated spin glass behavior in $\mathrm{Ni}_{1-x}\mathrm{Rh}_x$ [36]. However, our ac magnetic susceptibility measurements, presented in the Supplemental Material [27], show no evidence for spin glass behavior near T_C. Such a discrepancy may be due to different purity of starting materials or sample homogeneity.

For ferromagnets, the equation of state at T_C is given by $\Delta M \sim H^{1/\delta}$ [31]. From linear fits of $\log(\Delta M)$ vs $\log(\mu_0 H)$, as shown by the dashed line in Fig. 1(c), we determine that $T_C = 96$ K and $\delta \sim 3.5$ for the $x = 0.32$ sample. We applied the same analysis for all samples with $x = 0.30$–0.37. The critical exponents β and γ were determined by applying Arrott-Noakes scaling to the isotherms measured in the vicinity of T_C (see the Supplemental Material [27] for details) [31]. The composition dependence of all three exponents, δ, β, and γ, is summarized in Fig. 1(d). The Widom relation $\gamma/\beta = \delta - 1$ is obeyed over the entire range of Rh concentrations investigated here, a self-consistent check of the scaling analysis. At $x = 0.30$, which is well below x_{crit}, the exponents $\beta = 0.5$, $\gamma = 1.3$, and $\delta = 3.1$ are close to the expected mean-field values. With increasing x, the exponents deviate from the mean-field values and approach $\beta = 0.6$, $\gamma = 0.7$, and $\delta = 2.3$ at $x = 0.37$, just below x_{crit}. A similar evolution of the critical exponents with chemical substitution was observed in $\mathrm{Sr}_{1-x}\mathrm{Ca}_x\mathrm{RuO}_3$, where it was proposed that disorder resulted in enhanced quantum fluctuations near x_{crit} [37].

Zero field μSR measurements were performed on six samples of $\mathrm{Ni}_{1-x}\mathrm{Rh}_x$ with $x = 0.30$–0.39, in order to determine whether the magnetic order takes place via a first- or second-order process. Hallmarks of a first-order transition are phase separation or an abrupt change of ground state [22,38]. Conversely, in the case of a second-order transition, the size of the ordered moment is expected to continuously decrease without phase separation. μSR allows an independent measure of both the local order parameter and the magnetic volume fraction, f_{mag}, and can thus unambiguously distinguish between these scenarios. Representative muon decay asymmetry spectra, $P(t)$, are plotted in Fig. 2(a) for $x = 0.32$ at various temperatures below and above $T_C = 96$ K. Above T_C, $P(t)$ is essentially nonrelaxing, as expected in a PM state. The onset of magnetic order is signaled by a fraction of the asymmetry undergoing rapid relaxation at early times. The compositional dependence of $P(t)$ at $T = 2$ K is presented in Fig. 2(b). This comparison reveals that the samples with the highest Rh concentrations, $x = 0.375$ and 0.39 ($\geq x_{\text{crit}}$, blue and purple symbols), exhibit only weak relaxation down to the lowest measured temperatures, thus confirming the absence of magnetic order for these compositions. The samples with $x < x_{\text{crit}}$ exhibit sharp relaxation associated with magnetic order. The $P(t)$ data for all compositions and temperatures is well-described by the dynamic Kubo-Toyabe function [32]:

$$P(t) = (1 - f_{\text{mag}})e^{-\lambda t} + f_{\text{mag}}G_{\text{DKT}}(t, \sigma, \nu), \qquad (1)$$

where λ and σ are the relaxation rates for the nonmagnetic and magnetic fractions of the sample, respectively, and ν is the hopping rate. The temperature dependence of f_{mag} is presented in Fig. 2(c), revealing no evidence for phase separation; f_{mag} remains 100% up to Rh concentrations of $x = 0.36$ and drops to 0% at $x_{\text{crit}} = 0.375$. With increasing Rh concentration, the Kubo-Toyabe minimum moves to increasing times as can be seen in Fig. 2(b), consistent with a decreasing ordered moment. This suggests that the suppression of magnetic order in $\text{Ni}_{1-x}\text{Rh}_x$ occurs via a continuous second-order process.

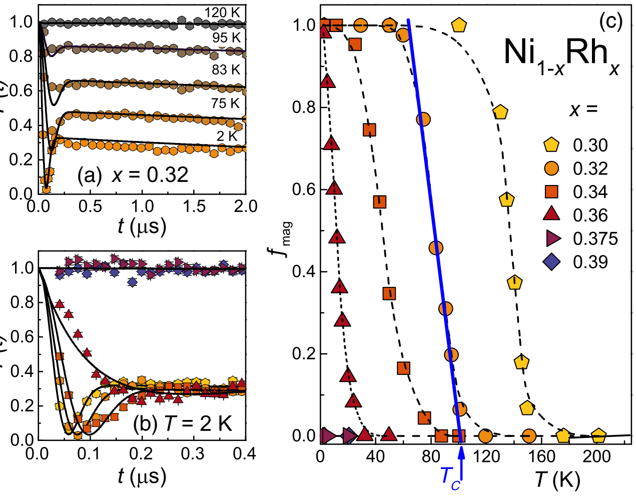

FIG. 2. (a) Temperature evolution of the normalized muon decay asymmetry $P(t)$ for $\text{Ni}_{1-x}\text{Rh}_x$ for $x = 0.32$. The solid lines are fits to Eq. (1). (b) $P(t)$ for all measured samples $x = 0.30$–0.39, at $T = 2$ K. (c) The magnetic volume fraction f_{mag} as a function of temperature. Solid line shows how T_C was determined.

Next we show evidence for divergent thermodynamic parameters in $\text{Ni}_{1-x}\text{Rh}_x$. Figure 3(a) shows the electronic specific heat C_{el}/T around $x_{\text{crit}} = 0.375$, where the phonon contribution has been subtracted from the measured specific heat. For concentrations that are both far above and far below x_{crit} ($x \leq 0.15$ and $x \geq 0.6$), C_{el}/T is nearly temperature-independent at low temperatures, as expected for a Fermi liquid (FL) [27]. Close to x_{crit}, C_{el}/T diverges logarithmically on cooling. The fastest divergence occurs at $x_{\text{crit}} = 0.375$, where $C_{\text{el}}/T = a_0 \log(T_0/T)$ between 0.1 and 3 K [solid line in Fig. 3(a)], such that a_0 is maximum at the QCP (red diamonds in Fig. 4). This logarithmic divergence was previously reported in $\text{Ni}_{0.62}\text{Rh}_{0.38}$ [39] and has also been observed in other QCP systems [9–11,40]. For $x > x_{\text{crit}}$, C_{el}/T levels off at the lowest temperatures, consistent with non-Fermi-liquid (NFL) to

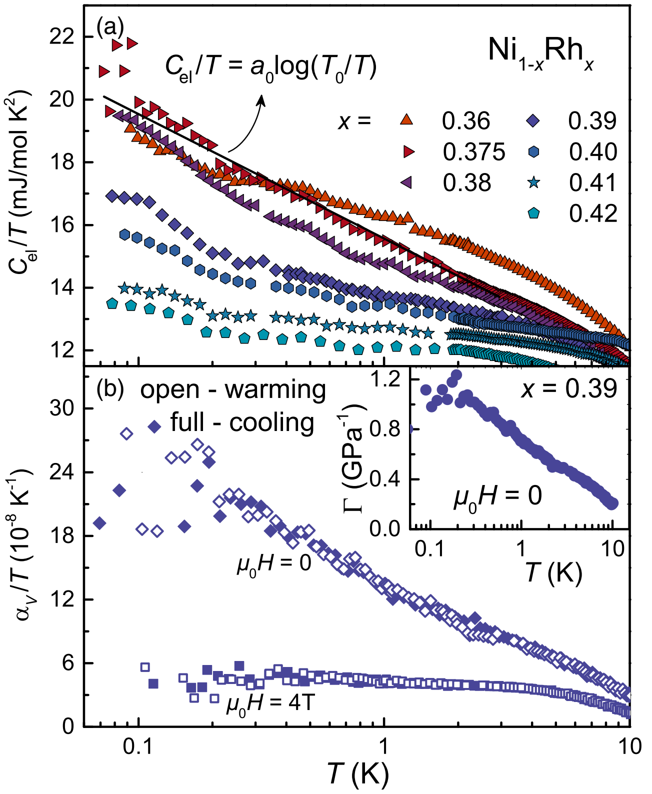

FIG. 3. (a) Temperature dependence of the electronic specific heat C_{el}/T for $\text{Ni}_{1-x}\text{Rh}_x$ with $x = 0.36$–0.42. The solid line represents a fit to $C_{\text{el}}/T = a_0 \log(T_0/T)$ at $x_{\text{crit}} = 0.375$. (b) The volume thermal expansion coefficient α_V/T at $\mu_0 H = 0$ (diamonds) and 4 T (squares) for $\text{Ni}_{1-x}\text{Rh}_x$ with $x = 0.39$. The inset shows the Grüneisen ratio Γ vs T at $\mu_0 H = 0$.

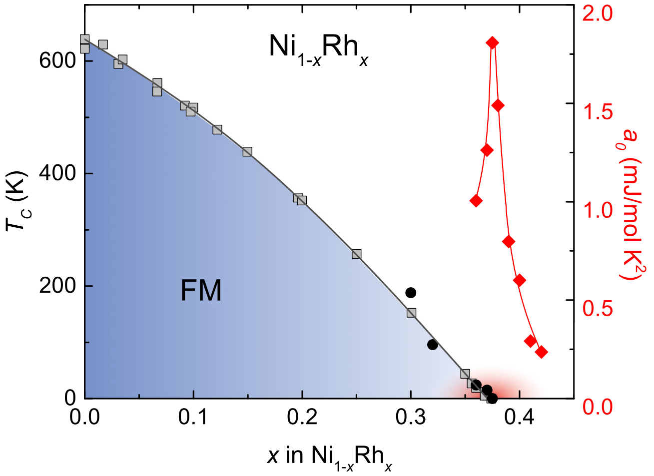

FIG. 4. $T_C - x$ phase diagram of Ni$_{1-x}$Rh$_x$. The blue region corresponds to long-range FM order. The red area marks the NFL behavior around the QCP. Black circles: T_C and red diamonds: the coefficient a_0 from the specific heat data (from current study). Gray squares: from Refs. [36,41–44].

FL crossover. This is similar to other FM and antiferromagnetic quantum critical systems [1,3–5].

QCPs are characterized by an accumulation of magnetic entropy S_{mag} as a function of the control parameter at low, but finite temperatures. In Ni$_{1-x}$Rh$_x$, this is underscored by the dependence of the specific heat parameter a_0 on x (red diamonds in Fig. 4), given that S_{mag} is commensurate to a_0, which, in turn, is maximum at the QCP. At the same time, S_{mag} is related to the volume thermal expansion α_V through the Maxwell relation $\alpha_V = -V^{-1}\partial S_{\mathrm{mag}}/\partial p$ (where p is pressure), and the divergence of α_V/T has been taken as proof of the QCP in heavy fermion systems, such as CeCu$_{6-x}$Au$_x$ [45], CeNi$_2$Ge$_2$, and YbRh$_2$(Si$_{0.95}$Ge$_{0.05}$)$_2$ [46]. Our data shows that at $x = 0.39$ (just above the QCP), zero-field α_V/T diverges logarithmically between 10 and 0.1 K [diamonds in Fig. 3(b)]. This is indicative of NFL behavior in proximity to the QCP [47]. The data show no hysteresis between heating (open) and cooling (full) measurements, ruling out any history-dependent spin glass effects. The length measurements on Ni$_{1-x}$Rh$_x$ with $x = 0.39$ reached the resolution limit of the dilatometer of $\Delta L \geq 10^{-3}$ Å at the lowest measured temperatures, resulting in an enhanced scattering below ~0.2 K. The application of a magnetic field of 4 T reduces α_V/T to a nearly constant value below 4 K, indicating a recovery of the FL behavior [squares in Fig. 3(b)]. This recovery of FL behavior is consistent with what has been observed in field-dependent specific heat measurements for Ni$_{0.62}$Rh$_{0.38}$ [39].

An additional probe for a QCP is the Grüneisen ratio $\Gamma = \alpha_V/C_{\mathrm{el}} \sim 1/E^* \cdot \partial E^*/\partial p$. Γ reveals the hydrostatic pressure dependence of the dominating, characteristic energy scale E^* (e.g., the energy related to the conduction band splitting at the Fermi energy, which is proportional to the spontaneous magnetization [48]). At a QCP, E^* vanishes, and Γ is expected to diverge with decreasing T [47]. In the low temperature range for the α_V measurements, the phonon contribution is negligible. The calculated Γ is depicted in the inset of Fig. 3(b), showing logarithmic divergence over two decades in temperature from $T = 10$ to 0.1 K. The fact that $\Gamma \sim -\log T$ suggests either that the quantum critical behavior in Ni$_{1-x}$Rh$_x$ extends to a finite pressure interval (rather than a point) [47], or that the system lies within a disordered quantum Griffiths phase [49].

We summarize the $T_C - x$ phase diagram of Ni$_{1-x}$Rh$_x$ in Fig. 4. Magnetization $M(T, H)$ and μSR measurements reveal the suppression of T_C with increasing Rh concentration up to $x_{\mathrm{crit}} = 0.375$ (black symbols). The magnetically ordered volume fraction remains 100% up to x_{crit}, while the magnitude of the ordered moment per formula unit continuously decreases, as expected for a second order transition [19]. In addition, the FM QCP is also revealed by the divergence of C_{el}/T, α_V/T, and Γ in the low temperature limit, associated with NFL behavior that extends up to ~10 K.

Finally, we compare our results with other Ni$_{1-y}M_y$ (M = Al, Si, V, Cr, Mn, Cu, Zn, Pd, and Sb) alloys. Nonmagnetic M metals dilute the Ni magnetic moment and therefore suppress the FM order. Magnetic susceptibility measurements on these alloys are sensitive to sample preparation [36,50]. In the absence of a spin glass state or short range order, the enhancement of C_{el}/T has been observed for all M where $T_C \to 0$ [50–52]. This commonality can be understood in terms of enhanced spin fluctuations and does not necessarily indicate quantum critical fluctuations. A noteworthy member of this family is Ni$_{1-y}$V$_y$ where V substitution results in quantum Griffiths effect that competes with critical behavior without reaching a QCP [53,54]. By contrast, Ni$_{1-x}$Rh$_x$ is the first member of the Ni$_{1-y}M_y$ family where divergent α_V/T and C_{el}/T result in divergent Γ [47], demonstrating the presence of a FM QCP. In fact, for most ferromagnets, when a dilution occurs in the magnetic sublattice, short-range order or spin glass behavior is observed [5]. The only exception is the 5f-electron system Th$_{1-x}$U$_x$Cu$_2$Si$_2$ that the FM transition remains continuous at the critical concentration, where NFL behavior is observed [55].

One plausible scenario to account for the FM QCP in Ni$_{1-x}$Rh$_x$ is the aforementioned BKV theory [6,16,17]. The current study utilized polycrystalline samples and the residual resistivity ratio (not shown), which is often taken as a gauge of the amount of disorder, is small and comparable among the whole series of Ni$_{1-x}$Rh$_x$. To test if the FM quantum criticality in Ni$_{1-x}$Rh$_x$ fulfills the universality class in the strong disorder regime of the BKV theory, the growth of single crystals is imperative and is the subject of an ongoing study. Ni$_{1-x}$Rh$_x$ shows the first occurrence of a FM QCP with dilution of the d-electron magnetic sublattice. This is in contrast with chemical substitution on the nonmagnetic sublattice in other FM QCP systems [9,10,18–21]. In particular, due to its chemical simplicity, $Ni_{1-x}Rh_x$ is an ideal platform for future studies and our work establishes a new approach to explore FM quantum criticality.

We acknowledge V. Taufour, D.-N. Cho, and D. Belitz for fruitful discussions. The work at Rice University was funded by the NSF DMR 1903741. We thank G. Costin for his assistance with EPMA measurements. The use of the EPMA facility at the Department of Earth, Environmental and Planetary Sciences, Rice University, is kindly acknowledged. We are grateful to Bassam Hitti and Gerald Morris for their assistance with the muon spin relaxation measurements. Research at McMaster University is supported by the Natural Sciences and Engineering Research Council of Canada. T. B. and T. S. are supported by Grant No. DE-SC0008832 from the Materials Sciences and Engineering Division in the U.S. Department of Energy's Office of Basic Energy Sciences and the National High Magnetic Field Laboratory through the NSF Cooperative Agreement No. DMR-1157490 and the State of Florida.

---

[*] clhuang1980@gmail.com

[1] H. v. Löhneysen, A. Rosch, M. Vojta, and P. Wölfle, Fermi-liquid instabilities at magnetic quantum phase transitions, Rev. Mod. Phys. **79**, 1015 (2007).

[2] E. Schuberth, M. Tippmann, L. Steinke, S. Lausberg, A. Steppke, M. Brando, C. Krellner, C. Geibel, R. Yu, Q. Si, and F. Steglich, Emergence of superconductivity in the canonical heavy-electron metal $YbRh_2Si_2$, Science **351**, 485 (2016).

[3] G. R. Stewart, Non-fermi-liquid behavior in d- and f-electron metals, Rev. Mod. Phys. **73**, 797 (2001).

[4] G. R. Stewart, Addendum: Non-fermi-liquid behavior in d- and f-electron metals, Rev. Mod. Phys. **78**, 743 (2006).

[5] M. Brando, D. Belitz, F. M. Grosche, and T. R. Kirkpatrick, Metallic quantum ferromagnets, Rev. Mod. Phys. **88**, 025006 (2016).

[6] D. Belitz, T. R. Kirkpatrick, and Thomas Vojta, First Order Transitions and Multicritical Points in Weak Itinerant Ferromagnets, Phys. Rev. Lett. **82**, 4707 (1999).

[7] S. Ran, C. Eckberg, Q.-P. Ding, Y. Furukawa, T. Metz, S. R. Saha, I.-L. Liu, M. Zic, H. Kim, J. Paglione, and N. P. Butch, Nearly ferromagnetic spin-triplet superconductivity, Science **365**, 684 (2019).

[8] D. A. Sokolov, M. C. Aronson, W. Gannon, and Z. Fisk, Critical Phenomena and the Quantum Critical Point of Ferromagnetic $Zr_{1-x}Nb_xZn_2$, Phys. Rev. Lett. **96**, 116404 (2006).

[9] S. Jia, P. Jiramongkolchai, M. R. Suchomel, B. H. Toby, J. G. Checkelsky, N. P. Ong, and R. J. Cava, Ferromagnetic quantum critical point induced by dimer-breaking in $SrCo_2(Ge_{1-x}P_x)_2$, Nat. Phys. **7**, 207 (2011).

[10] A. Steppke, R. Küchler, S. Lausberg, E. Lengyel, L. Steinke, R. Borth, T. Lühmann, C. Krellner, M. Nicklas, C. Geibel, F. Steglich, and M. Brando, Ferromagnetic quantum critical point in the heavy-Fermion metal $YbNi_4(P_{1-x}As_x)_2$, Science **339**, 933 (2013).

[11] E. Svanidze, L. Liu, B. Frandsen, B. D. White, T. Besara, T. Goko, T. Medina, T. J. S. Munsie, G. M. Luke, D. Zheng, C. Q. Jin, T. Siegrist, M. B. Maple, Y. J. Uemura, and E. Morosan, Non-Fermi Liquid Behavior Close to a Quantum Critical Point in a Ferromagnetic State Without Local Moments, Phys. Rev. X **5**, 011026 (2015).

[12] N. P. Butch and M. B. Maple, Evolution of Critical Scaling Behavior Near a Ferromagnetic Quantum Phase Transition, Phys. Rev. Lett. **103**, 076404 (2009).

[13] G. Abdul-Jabbar, D. A. Sokolov, C. D. O'neill, C. Stock, D. Wermeille, F. Demmel, F. Krüger, A. G. Green, F. Lévy-Bertrand, B. Grenier, and A. D. Huxley, Modulated magnetism in PrPtAl, Nat. Phys. **11**, 321 (2015).

[14] V. Taufour, U. S. Kaluarachchi, R. Khasanov, M. C. Nguyen, Z. Guguchia, P. K. Biswas, P. Bonfà, R. De Renzi, X. Lin, S. K. Kim, E. D. Mun, H. Kim, Y. Furukawa, C.-Z. Wang, K.-M. Ho, S. L. Bud'ko, and P. C. Canfield, Ferromagnetic Quantum Critical Point Avoided by the Appearance of Another Magnetic Phase in $LaCrGe_3$ Under Pressure, Phys. Rev. Lett. **117**, 037207 (2016).

[15] U. S. Kaluarachchi, S. L. Bud'ko, P. C. Canfield, and V. Taufour, Tricritical wings and modulated magnetic phases in $LaCrGe_3$ under pressure, Nat. Commun. **8**, 546 (2017).

[16] Y. Sang, D. Belitz, and T. R. Kirkpatrick, Disorder Dependence of the Ferromagnetic Quantum Phase Transition, Phys. Rev. Lett. **113**, 207201 (2014).

[17] T. R. Kirkpatrick and D. Belitz, Exponent relations at quantum phase transitions with applications to metallic quantum ferromagnets, Phys. Rev. B **91**, 214407 (2015).

[18] K. Huang, S. Eley, P. F. S. Rosa, L. Civale, E. D. Bauer, R. E. Baumbach, M. B. Maple, and M. Janoschek, Quantum Critical Scaling in the Disordered Itinerant Ferromagnet $UCo_{1-x}Fe_xGe$, Phys. Rev. Lett. **117**, 237202 (2016).

[19] T. Goko, C. J. Arguello, A. Hamann, T. Wolf, M. Lee, D. Reznik, A. Maisuradze, R. Khasanov, E. Morenzoni, and Y. J. Uemura, Restoration of quantum critical behavior by disorder in pressure-tuned (Mn,Fe)Si, npj Quantum Mater. **2**, 44 (2017).

[20] B. C. Sales, K. Jin, H. Bei, J. Nichols, M. F. Chisholm, A. F. May, N. P. Butch, A. D. Christianson, and M. A. McGuire, Quantum critical behavior in the asymptotic limit of high disorder in the medium entropy alloy $NiCoCr_{0.8}$, npj Quantum Mater. **2**, 33 (2017).

[21] Y. Lai, S. E. Bone, S. Minasian, M. G. Ferrier, J. Lezama-Pacheco, V. Mocko, A. S. Ditter, S. A. Kozimor, G. T. Seidler, W. L. Nelson, Y.-C. Chiu, K. Huang, W. Potter, D. Graf, T. E. Albrecht-Schmitt, and R. E. Baumbach, Ferromagnetic quantum critical point in $CePd_2P_2$ with Pd → Ni substitution, Phys. Rev. B **97**, 224406 (2018).

[22] Y. J. Uemura, T. Goko, I. M. Gat-Malureanu, J. P. Carlo, P. L. Russo, A. T. Savici, A. Aczel, G. J. MacDougall, J. A. Rodriguez, G. M. Luke, S. R. Dunsiger, A. McCollam, J. Arai, Ch. Pfleiderer, P. Böni, K. Yoshimura, E. Baggio-Saitovitch, M. B. Fontes, J. Larrea, Y. V. Sushko, and J. Sereni, Phase separation and suppression of critical dynamics at quantum phase transitions of mnsi and $Sr_{1-x}Ca_xRuO_3$, Nat. Phys. **3**, 29 (2007).

[23] C. L. Huang, D. Fuchs, M. Wissinger, R. Schneider, M. C. Ling, M. S. Scheurer, J. Schmalian, and H. v. Löhneysen, Anomalous quantum criticality in an itinerant ferromagnet, Nat. Commun. **6**, 8188 (2015).

[24] Y. Kraftmakher, Curie point of ferromagnets, Eur. J. Phys. **18**, 448 (1997).

[25] E. Bucher, W. F. Brinkman, J. P. Maita, and H. J. Williams, Magnetic Susceptibility and Specific Heat of Nearly Ferromagnetic NiRh Alloys, Phys. Rev. Lett. **18**, 1125 (1967).

[26] J.-W. Yeh, S.-K. Chen, S.-J. Lin, J.-Y. Gan, T.-S. Chin, T.-T. Shun, C.-H. Tsau, and S.-Y. Chang, Nanostructured high-entropy alloys with multiple principal elements: Novel alloy design concepts and outcomes, Adv. Eng. Mater. **6**, 299 (2004).

[27] See the Supplemental Material at http://link.aps.org/supplemental/10.1103/PhysRevLett.124.117203 for details of sample preparation, ac magnetic susceptibility, Arrott-Noakes scaling, μSR, and phonon contributions to the specific heat, which includes Refs. [28–34].

[28] Kenny Ståhl, https://www.kemi.dtu.dk/english/research/physicalchemistry/protein_og_roentgenkrystallografi/computer_programs.

[29] F. Hofer, Thermodynamic properties of solid rhodium-nickel alloys, J. Solid State Chem. **45**, 303 (1982).

[30] L. Vegard, Die konstitution der mischkristalle und die raumfüllung der atome, Z. Phys. **5**, 17 (1921).

[31] A. Arrott and J. E. Noakes, Approximate Equation of State for Nickel Near Its Critical Temperature, Phys. Rev. Lett. **19**, 786 (1967).

[32] R. Kubo and T. Toyabe, Magnetic resonance and relaxation, in *Proceedings of the XIVth Colloque Ampere Ljubljana*, edited by R. Blinc (Amsterdam, North-Holland Publ. Co., 1967), p. 810.

[33] M. L. G. Foy, Neil Heiman, W. J. Kossler, and C. E. Stronach, Precession of Positive Muons in Nickel and Iron, Phys. Rev. Lett. **30**, 1064 (1973).

[34] B. D. Patterson, K. M. Crowe, F. N. Gygax, R. F. Johnson, A. M. Portis, and J. H. Brewer, Precession of $\mu+$ in single crystal nickel, Phys. Lett. **46A**, 453 (1974).

[35] J. M. Santiago, C.-L. Huang, and E. Morosan, Itinerant magnetic metals, J. Phys. Condens. Matter **29**, 373002 (2017).

[36] D. W. Carnegie and H. Claus, Magnetism and atomic short-range order in Ni-Rh alloys, Phys. Rev. B **30**, 407 (1984).

[37] D. Fuchs, M. Wissinger, J. Schmalian, C.-L. Huang, R. Fromknecht, R. Schneider, and H. v. Löhneysen, Critical scaling analysis of the itinerant ferromagnet $Sr_{1-x}Ca_xRuO_3$, Phys. Rev. B **89**, 174405 (2014).

[38] B. A. Frandsen, L. Liu, S. C. Cheung, Z. Guguchia, R. Khasanov, E. Morenzoni, T. J. S. Munsie, A. M. Hallas, M. N. Wilson, Y. Cai *et al.*, Volume-wise destruction of the antiferromagnetic Mott insulating state through quantum tuning, Nat. Commun. **7**, 12519 (2016).

[39] B. B. Triplett and N. E. Phillips, Low-temperature heat capacity of $Ni_{0.62}Rh_{0.38}$, Phys. Lett. **37A**, 443 (1971).

[40] M. Brando, W. J. Duncan, D. Moroni-Klementowicz, C. Albrecht, D. Grüner, R. Ballou, and F. M. Grosche, Logarithmic Fermi-Liquid Breakdown in $NbFe_2$, Phys. Rev. Lett. **101**, 026401 (2008).

[41] W. C. Muellner and J. S. Kouvel, Magnetic properties of Ni-Rh alloys near the critical composition for ferromagnetism, Phys. Rev. B **11**, 4552 (1975).

[42] H. Fujiwara, H. Kadomatsu, K. Ohishi, and Y. Yamamoto, Effects of hydrostatic pressure on the Curie temperature of Ni-based alloys (Ni-V, -Cu, -Pd, -Pt and -Rh), J. Phys. Soc. Jpn. **40**, 1010 (1976).

[43] R. Vetter and J. Vuik, Resistivity and curie point of NiRh alloys, Phys. Status Solidi (A) **63**, 637 (1981).

[44] H. P. Wijn, Magnetic Properties of Metals—d-Elements, *Alloys and Compounds* (Springer-Verlag, Berlin Heidelberg, 1991).

[45] K. Grube, S. Zaum, O. Stockert, Q. Si, and H. v. Löhneysen, Multidimensional entropy landscape of quantum criticality, Nat. Phys. **13**, 742 (2017).

[46] R. Küchler, N. Oeschler, P. Gegenwart, T. Cichorek, K. Neumaier, O. Tegus, C. Geibel, J. A. Mydosh, F. Steglich, L. Zhu, and Q. Si, Divergence of the Grüneisen Ratio at Quantum Critical Points in Heavy Fermion Metals, Phys. Rev. Lett. **91**, 066405 (2003).

[47] L. Zhu, M. Garst, A. Rosch, and Q. Si, Universally Diverging Grüneisen Parameter and the Magnetocaloric Effect Close to Quantum Critical Points, Phys. Rev. Lett. **91**, 066404 (2003).

[48] P. Mohn, *Magnetism in the Solid State: An Introduction* (Springer, Berlin, 2006).

[49] T. Vojta, Thermal expansion and Grüneisen parameter in quantum Griffiths phases, Phys. Rev. B **80**, 041101(R) (2009).

[50] I. P. Gregory and D. E. Moody, The low temperature specific heat and magnetization of binary alloys of nickel with titanium, vanadium, chromium and manganese, J. Phys. F **5**, 36 (1975).

[51] K. P. Gupta, C. H. Cheng, and P. A. Beck, Low-temperature specific heat of Ni-base fcc solid solutions with Cu, Zn, Al, Si, and Sb, Phys. Rev. **133**, A203 (1964).

[52] M. Nicklas, M. Brando, G. Knebel, F. Mayr, W. Trinkl, and A. Loidl, Non-Fermi-Liquid Behavior at a Ferromagnetic Quantum Critical Point in $Ni_{1-x}Pd_x$, Phys. Rev. Lett. **82**, 4268 (1999).

[53] S. Ubaid-Kassis, T. Vojta, and A. Schroeder, Quantum Griffiths Phase in the Weak Itinerant Ferromagnetic Alloy $Ni_{1-x}V_x$, Phys. Rev. Lett. **104**, 066402 (2010).

[54] T. Vojta, Quantum Griffiths effects and smeared phase transitions in metals: Theory and experiment, J. Low Temp. Phys. **161**, 299 (2010).

[55] M. Lenkewitz, S. Corsépius, G.-F. v. Blanckenhagen, and G. R. Stewart, Heavy non-fermi-liquid behavior in nearness to ferromagnetism in $Th_{1-x}U_xCu_2Si_2$, Phys. Rev. B **55**, 6409 (1997).